

Parametric neutronics analyses of lattice geometry and coolant candidates for a soluble-boron-free civil marine SMR core using micro-heterogeneous duplex fuel

Syed Bahauddin Alam^{a,*}, Cameron S. Goodwin^b, Geoffrey T. Parks^a

^a*Department of Engineering, University of Cambridge
Cambridge, CB2 1PZ, United Kingdom*

^b*Rhode Island Atomic Energy Commission
16 Reactor Rd, Narragansett, RI 02882, USA*

Abstract

Civilian marine reactors face a unique set of design challenges in addition to the usual irradiation and thermal-hydraulic limits affecting all reactors. These include requirements for a small core size, long core lifetime, a 20% cap on fissile loading, and limitations on the use of soluble boron. One way to achieve higher burnup/longer core life is to alter the neutron spectrum by changing the hydrogen-to-heavy-metal ratio, thus increasing the conversion of fertile isotopes in the fuel. In this reactor physics study, we optimize the two-dimensional lattice geometry of a 333 MWth soluble-boron-free marine PWR for 18% ²³⁵U enriched micro-heterogeneous ThO₂-UO₂ duplex fuel and 15% ²³⁵U enriched homogeneously mixed all-UO₂ fuel. We consider two types of coolant: H₂O and mixed 80% D₂O + 20% H₂O. We aim to observe in which spectrum discharge burnup is maximized in order to improve uranium utilization, while satisfying the constraint on moderator temperature coefficient. It is observed that higher discharge burnup for the candidate fuels is achievable by using either a wetter lattice or a much drier lattice than normal, while epithermal lattices are distinctly inferior performers. The thorium-rich duplex fuel exhibits higher discharge burnup potential than the all-UO₂ fuel for all moderation regimes for both coolants. The candidate fuels exhibit higher initial reactivity and discharge burnup with the mixed D₂O-H₂O coolant than with the H₂O coolant in the under-moderated regime, whereas these values are lower for the D₂O-H₂O coolant in the over-moderated regime.

Keywords: Civil marine propulsion, Small modular reactor, Soluble-boron-free operation, Micro-heterogeneous thorium-based duplex fuel, Lattice geometry optimization, Achievable discharge burnup, Initial reactivity, Conversion ratio, Moderator temperature coefficient.

*Corresponding author

Email address: syed.nuclear@cantab.net (Syed Bahauddin Alam)

1. Introduction

Perhaps surprisingly, interest is presently being shown in the possible application of nuclear energy in marine propulsion and this topic has recently received renewed attention after many years of apparent neglect (Hirdaris et al., 2014, Ragheb, 2012, Carlton et al., 2011, Sawyer et al., 2008). Since 2002 there has been a resurgence of reconsidering the technical and economic feasibility of technology options for marine nuclear propulsion due to the environmental concerns and changes in market economics. A nuclear-powered ship – be it a surface ship or a submarine – receives its propulsion energy from a nuclear power plant on board, and can be dubbed an “atomic engine” (Ragheb, 2012). The main advantages of nuclear marine propulsion are that atomic engines do not consume hydrocarbon-based fuel and oxygen, and produce no exhaust gas (Ragheb, 2012). Atomic engines are reliable, compact sources of energy that can operate for years without new fuel (Hirdaris et al., 2014). These benefits have motivated the development of atomic engines without too much concern regarding cost (Hirdaris et al., 2014, Carlton et al., 2011, Sawyer et al., 2008). The employment of advanced reactors and a careful concentration on cost-conscious design can result in nuclear marine propulsion systems that are economically superior to conventional energy systems.

In an effort to decarbonise energy production and concerns about the effects of climate change, there is growing interest in the possibility of using nuclear propulsion systems (Kramer, 1962). Maritime shipping accounts for $\sim 3\%$ of global CO_2 emissions, and could account for 15-30% of all CO_2 emissions permitted in 2050 as economic growth in the developing world increases the volume of international commerce. The current global shipping industry emits roughly 1Gt CO_2 about a third more than current aviation emissions. Without significant policy action, future projections of global maritime shipping emissions suggest that we are likely to be on a path that would lead to global shipping emissions of ~ 3 Gt CO_2 in 2050. This would represent almost a threefold increase on today’s levels (1Gt CO_2). Diesel shipping poses serious threats to the environment both on inland waterways and on the ocean. Most large ships emit significant amounts of sulphur and nitrous oxides from the combustion of heavy fuel oil, and it is expected that maritime sources will soon account for the majority of all SO_x and NO_x emissions in Europe (Otto, 2013, Hirdaris et al., 2014). These pollutants are solely responsible for additional health costs of tens of billions of euros associated with heavy maritime traffic (Otto, 2013, Schinas and Stefanakos, 2012). Since nuclear fission produces no direct emissions, it clearly enjoys key environmental advantages over current diesel engines.

Considering the non-proliferation issues associated with naval reactors, a major loophole has been created by the Non-Proliferation Treaty (NPT) of nuclear weapons which allows a non-nuclear-weapon country to avoid international safeguards governing highly enriched weapon-grade fissile materials if it claims that the materials will be used for a nuclear marine propulsion program (McCord, 2013, Harvey, 2010). Therefore, a non-nuclear-weapon country can produce or stockpile weapons-grade highly enriched uranium (HEU) for a nuclear marine propulsion core to be constructed in the future, which can then potentially be used for the production of nuclear weapons. Concerns regarding nuclear weapons proliferation

43 have significantly increased since some countries have sought to develop new nuclear energy
44 programs, and it is well known that these countries can use centrifuges to make HEU more
45 easily than previously assumed (McCord, 2013, Ma and Von Hippel, 2001). However, in
46 recent times, there have been significant technological advances in low enrichment uranium
47 (LEU) fuel systems and efforts made to improve LEU fuel technology in major universities
48 and R&D departments of leading nuclear laboratories (Alam, 2018). Therefore, in light of
49 the proliferation concerns, there is a strong motivation to examine the design of marine
50 reactor cores with the low-enriched uranium (LEU) fuel candidates.

51 There are several engineering challenges unique to civil marine reactors (Ragheb, 2012).
52 Civil marine reactors must additionally be capable of operating with long refueling intervals
53 and low fissile loadings (Hirdaris et al., 2014), which makes it fundamentally different from
54 land-based nuclear plant system. In previous studies (Alam, 2018, Alam et al., 2019) we have
55 examined the feasibility of micro-heterogeneous ThO₂-UO₂ duplex fuel and all-UO₂ fuel for
56 civil marine propulsion. We sought to design 333 MW thermal power cores that will operate
57 with long refueling intervals of (at least) 15 effective-full-power-years (EFPY). We focus on
58 PWR technology since this is the most common reactor in the world today, with a proven
59 record of maritime operation. PWRs are robust and proven reactors for aircraft carrier and
60 submarine propulsion. Therefore, a PWR type small modular reactor (SMR) is considered in
61 this study. In addition, for reasons of operational simplicity, there is no soluble boron used
62 in naval reactors. The elimination of soluble boron offers several advantages for reactor cores.
63 Most of these advantages are realized through significant core simplification (removal of
64 pipes, pumping, and purification systems), space saving, the removal of the corrosive effects
65 of soluble boron over the long core life, and from improved safety effects, improvement of
66 the moderator temperature coefficient and elimination of an entire class of boron dilution
67 accidents (Kim et al., 1998). Additionally, there is concern that if a ship relying on soluble
68 boron for reactivity control were to sink, the dilution of the coolant with seawater could
69 cause a criticality accident (Kusunoki et al., 2000).

70 In this study, we seek to optimize the two-dimensional lattice geometry of a 333 MWth
71 SBF marine PWR, with an emphasis on the initial reactivity, achievable discharge burnup
72 and conversion ratio, using 18% ²³⁵U enriched micro-heterogeneous ThO₂-UO₂ duplex fuel
73 and 15% ²³⁵U enriched homogeneously mixed all-UO₂ fuel. One way to achieve higher
74 burnup/longer core life is to alter the neutron spectrum by changing the hydrogen-to-heavy-
75 metal ratio (H/HM), thus increasing the conversion of fertile isotopes in the fuel (Otto, 2013,
76 Xu, 2003, Alam et al., 2016). We have considered two types of coolant: H₂O and a mixture
77 of 80% D₂O + 20% H₂O. To date, mixing light and heavy D₂O waters as a “mixed coolant”
78 isn’t practically employed (Nagy et al., 2014), although some proposed reactor designs, such
79 as Spectral Shift Control Reactor (SSCR) (Engelder, 1961) and the Mixed Moderator PWR
80 (MPWR) (Tochihara et al., 1998) considered this technique. In addition, for the H₂O coolant,
81 important contributions are made by an MIT study (Xu, 2003), where optimization of the
82 PWR lattice is performed for a range of H/HM. This study explored how many different
83 independent variables affect discharge burnup and what types of H/HM are most effective
84 for maximizing burnup. However, this analysis assumed licensing limits of 5% enrichment
85 with soluble boron system.

86 There is a significant gap in assessing the effect of neutron spectrum variation over burnup,
 87 especially for SBF, SMR cores (Alam, 2018, Otto, 2013, Ippolito, 1990). Therefore, the main
 88 objective of this parametric neutronic study is to observe the effects of varying the neutron
 89 spectrum under different degrees of moderation in order to maximize the attainable discharge
 90 burnup (thereby improving uranium utilisation) while maintaining a negative moderator
 91 temperature coefficient (MTC). It is important to address that since the scope of this paper
 92 is limited to “parametric neutronic analyses”, the safety issues (thermal-hydraulics, fuel
 93 performance) are out of the scope of this paper.

94 2. Design methods

95 2.1. Reference subassembly sizing

96 Our subassembly sizing calculations use a 13×13 assembly design. For purposes of
 97 comparison, we began by considering a standard Westinghouse 4-loop PWR core, which has
 98 a fueled core area of 8.9 m^2 and uses 193 assemblies with 264 pins in a 17×17 array (Winters,
 99 2004). We found that the marine reactor requires a fueled core area of 3 m^2 , a 67% reduction
 100 in area (Alam, 2018, Alam et al., 2015, Otto, 2013). If 112 assemblies with a 13×13 pin
 101 array are used, we achieve this size reduction while reducing the freedom for subassembly
 102 design and core design equally (a 42% reduction in pins per assembly and a 42% reduction
 103 in assemblies per core). Fortuitously, 112 is a ‘magic number’ of squares that can be formed
 104 into the approximate shape of a circle (Fig. 1b). Thus, we begin with 112 assemblies with a
 105 13×13 arrangement. In a Westinghouse 17×17 assembly, there are 24 control pins and one
 106 instrument tube (8.7% of pin locations). We maintain a similar ratio in our design, while
 107 preserving octant symmetry to help reduce power peaking, so we have 16 control pins (9.5%
 108 of pin locations) and 153 fueled pins.

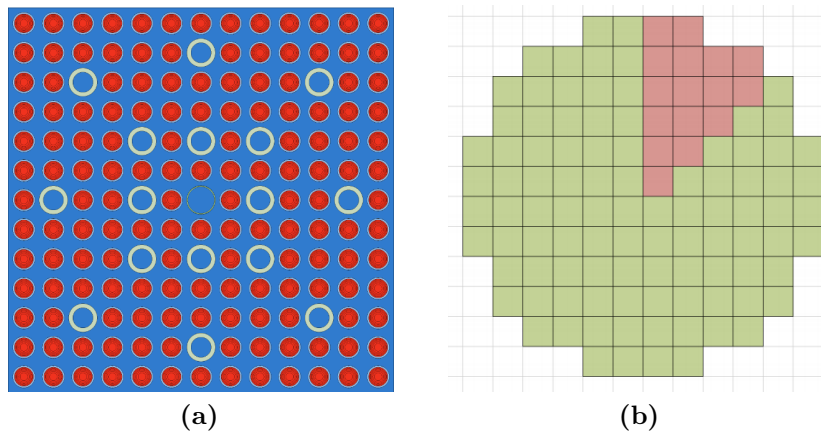


Fig. 1. Subassembly sizing: (a) 13×13 assembly geometry layout; (b) Schematic of a 112-assembly core, with one octant highlighted.

109 *2.2. Computational methods*

110 The subassembly design analysis employed the WIMS-10 lattice physics code using nuclear
 111 data from the JEF 2.2 database available from the IAEA (Newton et al., 2008). For each
 112 burnup step, WIMS completes a 172-group ‘fine’ solution to the transport equation in a
 113 smeared geometry. It then refines this solution using a few-group calculation in a precise
 114 geometry. In this study, we used a 6 energy group structure, as shown in Table 1. It is
 115 important to address the calculation route for WIMS. In our study, WIMS module HEAD
 116 sets up cross-sections in library groups and PRES/CACTUS/RES sequence does a subgroup
 117 calculation of resonance shielding, where PRES sets up subgroup cross-sections at the fuel
 118 temperature, CACTUS calculates the subgroup fluxes by Method of Characteristics (MoC)
 119 and RES completes the subgroup calculation of resonance shielding. Multicell collision
 120 probability equations is solved by PERSEUS/PIP sequence. PERSEUS calculates multicell
 121 collision probabilities for the full problem in the geometry and PIP calculates neutron spectra
 122 for each material. The condensed cross-sections and flux spectrum calculated by COND
 123 module. BURNUP module carries out depletion of fuel at specified rating and timestep.

Group	1	2	3	4	5	6
Upper fine group	1	23	46	93	136	153
Lower fine group	22	45	92	135	152	172
Upper (eV)	19.64×10^6	820.85×10^3	9.12×10^3	4.00	625×10^{-3}	140×10^{-3}
Lower (eV)	820.85×10^3	9.12×10^3	4.00	625×10^{-3}	140×10^{-3}	110×10^{-6}

Table 1. 6-group WIMS energy structure.

124 *2.3. Fuel selection*

125 There have been several past studies of homogeneously mixed Th/UO₂ fuel (Galperin
 126 et al., 2002) and heterogeneous seed-blanket arrangements (Kazimi et al., 1999, Todosow
 127 et al., 2005, Clayton, 1993). Homogeneously mixed Th/UO₂ fuel only yields promising
 128 performance in a single-batch core when the ²³⁵U enrichment exceeds 20% (Galperin et al.,
 129 2002, Otto, 2013). Previous studies have indicated that thorium’s advantages are best
 130 realized in micro-heterogeneous and heterogeneous geometries (MacDonald and Lee, 2004),
 131 but heterogeneous seed-blanket arrangements rely on being able to remove the seed region
 132 and replace it mid-life with fresh fuel (Kazimi et al., 1999, Todosow et al., 2005, Clayton,
 133 1993), which is not compatible with single-batch operation. In contrast, the ability of duplex
 134 fuel to exploit the potential benefits of thorium in the context of a single-batch, low enriched
 135 uranium, SBF, long-life, small modular reactor (SMR) core is yet to be fully explored (Zhao,
 136 2001, MacDonald and Lee, 2004). Therefore, in this study we evaluate the performance of
 137 micro-heterogeneous ThO₂-UO₂ duplex fuel¹, loaded in a single-batch strategy. To provide a
 138 basis for comparison we also evaluate the performance of homogeneously mixed all-UO₂ fuel.

¹We use the term ‘duplex’ to refer to the micro-heterogeneous ThO₂-UO₂ duplex fuel throughout this paper.

139 *2.4. Design of fissile loading*

140 In ThO₂-UO₂ duplex fuel, the UO₂ and ThO₂ components are not blended together (as
141 in homogeneous fuel) but are discretely interspersed on small distance scales (Alam et al.,
142 2019, Shwageraus et al., 2004, Alam et al., 2018c,d). In our case, an individual fuel pin is
143 composed of a UO₂ centre surrounded by an annulus of pure ThO₂, as shown in Fig. 2.

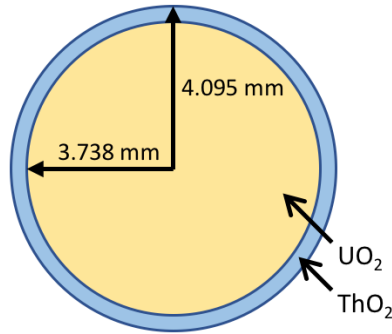
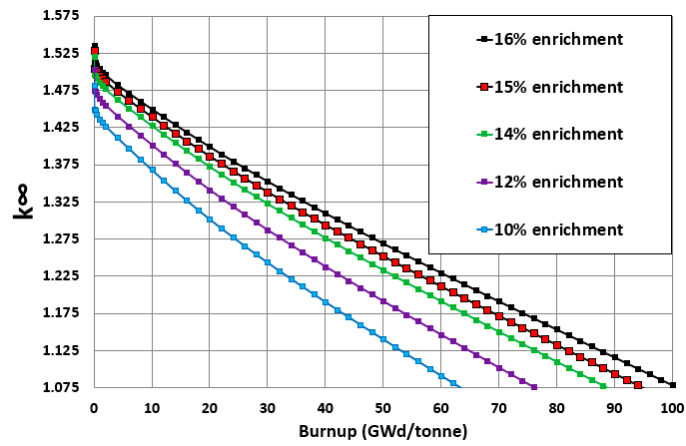


Fig. 2. Configuration of the micro-heterogeneous duplex ThO₂-UO₂ fuel.

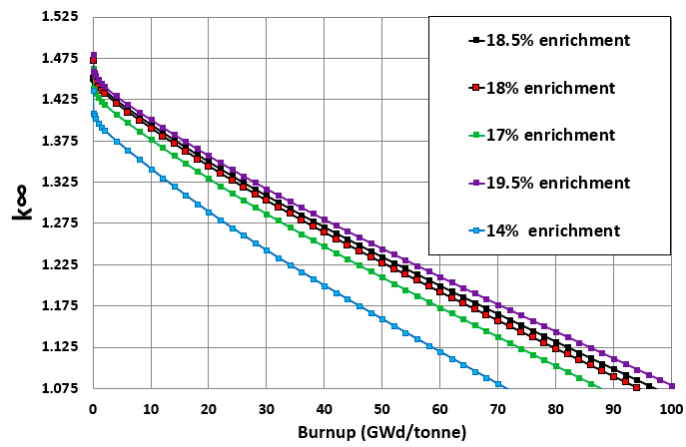
144 It was assumed in the sizing analysis that the irradiation tolerance of the fuel (100
145 GWd/tonne) is the primary limiting factor in the core design. According to an MIT study
146 (Xu, 2003), smaller cores are more sensitive to higher neutron leakage than that of the
147 commercial PWR. As an example, for constant power density, a 500 MWth core will exhibit
148 approximately twice leakage than that of the 3500 MWth core. The smaller core (500 MWth)
149 will lose 7%, If the latter (3500 MWth) loses 3.5%. Furthermore, a recent SMR neutronic
150 study by Oak Ridge National Lab (Brown et al., 2017) showed that ~400 MWth SMR
151 exhibits 6–8% leakage depending on the core loading patters and other input parameters.
152 Since WIMS calculations assume an infinitely-large core and a small core is prone to larger
153 leakage, we have assumed 7.5% leakage in this study.

154 In conventional PWR reactor, 4% leakage is considered while considering 2D lattice-level
155 calculations (Alam, 2018). We have estimated from our core sizing analyses that considering
156 our marine propulsion SMR core (Power = 333 MWth, Volume = 5.3 m³), leakage of 7.5% is
157 considered conservative. This leakage has been checked with 3D whole-core nodal diffusion
158 code PANTHER (Hutt, 1992). In the assembly level analysis for fresh fuel in WIMS (which
159 assumes an infinitely-large core), discharge burnup is 95 GWd/tonne considering 7.5% leakage,
160 while whole-core exhibits the average burnup of 97 GWd/tonne, which proves that 7.5%
161 leakage is conservative for our SMR core design. The discharge burnup is therefore estimated
162 from the point on the assembly burnup curve where the infinite multiplication factor, k_{∞} , is
163 1.075.

164 The fissile loadings of the duplex and UO₂ fuels were determined from enrichment
165 sensitivity studies, seeking values that keep the core critical for a burnup of ~95 GWd/tonne.
166 It is clear from Figs. 3a and 3b that, in order to achieve the target discharge burnup, initial
167 enrichments of 15% and 18% ²³⁵U are required for the UO₂ and duplex fuels, respectively.
168 The duplex fuel requires higher enrichment than the all-UO₂ fuel due, in part, to the lower



(a)



(b)

Fig. 3. Fuel depletion calculations for various fissile loadings: (a) UO_2 fuel; (b) Duplex fuel.

169 volume of UO_2 in the fuel and, in part, to the higher thermal absorption cross-section of the
 170 fertile ^{232}Th .

171 Lattice physics calculations for the assemblies were performed in previous studies ([Almu-](#)
 172 [tairi et al., 2018](#), [Alam et al., 2018b,a](#)) using the deterministic transport code WIMS, the
 173 Monte Carlo (MC) code Serpent ([Leppänen and Pusa, 2009](#)) and the hybrid MC code MONK
 174 ([Long et al., 2015](#)). For both candidate fuels, excellent agreement ($\sim 100\text{--}350$ pcm) was
 175 observed between the codes, giving reassurance that WIMS can be used to provide reliable
 176 lattice physics results for SBF marine propulsion cores at much reduced computational cost
 177 compared to the MC code Serpent and hybrid MC code MONK.

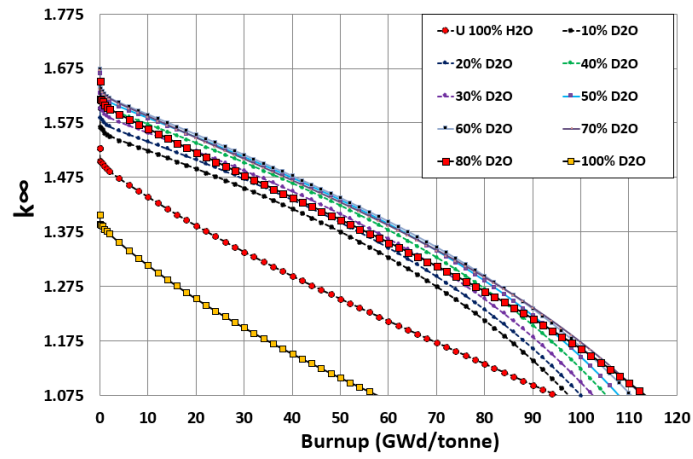
178 *2.5. Coolant molecular ratios*

179 Next, we use mixtures of light and heavy water at molecular ratios ranging from 0%
 180 to 100% D_2O with both candidate fuels. Figs. [4a](#) and [4b](#) show that both fuels achieve the
 181 highest discharge burnup with the 80% D_2O + 20% H_2O mixed coolant. Neutron capture in
 182 D_2O - H_2O dominates when it is more than 80% D_2O due to the substantial degradation in
 183 the thermal neutron utilization arising from the reduced presence of hydrogen atoms. This
 184 necessarily provides the highest uranium utilization, making this coolant composition the
 185 natural choice to take forward in this study. As expected, since deuterium is not as efficient a
 186 neutron moderator as hydrogen, the neutron spectrum was found to be increasingly hardened
 187 and the resonance flux relatively higher as the D_2O percentage in the moderator increased.

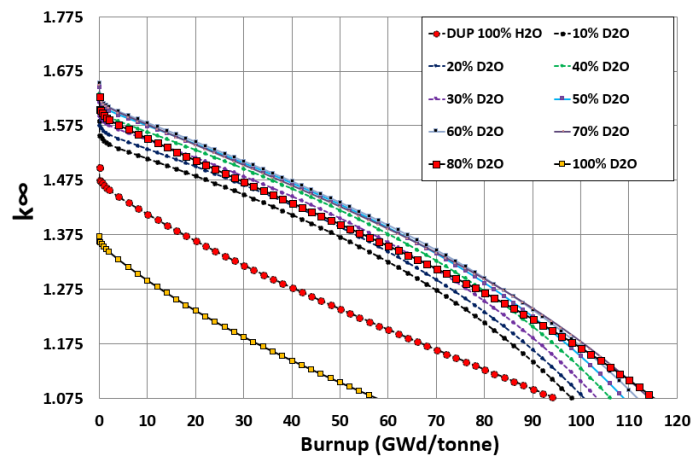
188 The reference design parameters of the proposed marine core are shown in Table 2 ([Alam,](#)
 189 [2018](#)).

Parameter	Value
Thermal power (MWth)	333.33
Minimum desired lifetime (years)	15
Assembly size	13×13
Control rods per assembly	16
Pin pitch (mm)	12.65
Fuel pellet diameter (mm)	8.19
Cladding thickness (mm)	0.605
Gap thickness (mm)	0.0498
Number of assemblies	112
Fuel height (m)	1.79
Core diameter (m)	1.97
Pitch/diameter ratio	1.33
Hydrogen-to-heavy metal (H/HM) ratio	3.99
Assembly side length (cm)	16.45
Assembly area (m^2)	0.03
Power density (MW/m^3)	63
Average linear rating (kW/m)	10

Table 2. Reference design parameters of proposed marine core.



(a)



(b)

Fig. 4. Fuel depletion calculations for varying molecular ratios of light and heavy water: (a) 15% ^{235}U enriched UO_2 fuel; (b) 18% ^{235}U enriched duplex fuel.

190 3. Lattice geometry optimization and moderation effects

191 The main objective of this parametric study is to observe the effects of varying the neutron
192 spectrum under different degrees of moderation in order to maximize the attainable discharge
193 burnup and secure improved uranium utilization while maintaining a negative MTC. Since
194 the achievable burnup is dependent on the hydrogen-to-heavy-metal ratio (H/HM) for H₂O
195 coolant, and on the deuterium-hydrogen/heavy-metal ratio (DH/HM) for mixed D₂O-H₂O
196 coolant, we optimize these ratios by changing: (1) the fuel rod diameter; (2) the pin pitch;
197 and (3) the coolant density. Together, these parameters determine the reactor’s H/HM and
198 DH/HM ratios, and hence have a crucial effect on the neutron energy spectrum.

199 Our strategy for this study of moderation effects is the following: by varying the H/HM
200 and DH/HM ratio in a core, we can find the most suitable operating range with respect to
201 achievable discharge burnup for a given initial enrichment for the candidate fuels. Optimizing
202 moderation to achieve long core life requires a balance to be struck between three main
203 factors (Alam, 2018):

- 204 (a) Early in life, it is desirable to encourage a higher neutron capture rate in the fertile
205 components of the fuel, suppressing initial reactivity and enhancing the breeding of new
206 fissile material.
- 207 (b) Late in life, it is necessary to reduce captures in the fertile components of the fuel so as
208 to increase the core reactivity, which helps in preventing the core from losing criticality.
- 209 (c) And throughout all stages of life, it is necessary to maintain a sufficiently negative MTC
210 to ensure stable operation.

211 In this study, we have defined the following:

- 212 1. The fast region to correspond to a H/HM or DH/HM < 0.50 , the epithermal region to
213 H/HM or DH/HM between 0.50 and 2.88, and the thermal region to H/HM or DH/HM
214 > 2.88 (Xu and Driscoll, 1997, Alam, 2018).
- 215 2. We refer to the region below the optimal (point of highest discharge burnup) H/HM or
216 DH/HM as ‘under-moderated’ and the region above the optimum as ‘over-moderated’.
- 217 3. The reference values of pin pitch = 12.65 mm, fuel pin diameter = 9.50 mm, coolant
218 density = 0.707 g/cm³ (for H₂O) and 1.0832 g/cm³ (for 80% D₂O + 20% H₂O).

219 We use ‘D₂O’ as a short-hand label for the 80% D₂O + 20% H₂O coolant².

220 3.1. Initial reactivity

221 The focus here is on the beginning-of-life (BOL) k_{∞} of poison-free fuel lattices at hot
222 full power and xenon-free conditions. We have investigated BOL k_{∞} by varying the coolant
223 density, fuel pin diameter and pin pitch over wide ranges with other parameters held constant.
224 These resulting plots provide information on several points of interest.

225 Fig. 5a shows that an increase in H/HM leads to a higher BOL k_{∞} for both the duplex
226 and all-UO₂ fuels up to some value of H/HM. Due to the increased presence of hydrogen

²80% D₂O + 20% H₂O coolant is referred to interchangeably as ‘mixed coolant’ and ‘D₂O’.

atoms, neutrons are better thermalized (Fig. 5b) up to $H/HM \approx 15$ for H_2O coolant. k_∞ peaks at this H/HM value and tends to decrease thereafter. In the over-moderated region, k_∞ decreases as H/HM increases since the large capture cross-section of water begins to dominate the effect of improved neutron thermalization (Xu and Driscoll, 1997). It should be noted that our reference marine PWR lattice has H/HM and DH/HM values of 3.99 and 5.0, respectively and therefore is not optimal if trying to maximize BOL k_∞ .

Figs. 6a and 6b show that the variation of BOL k_∞ for the candidate fuels is similar with the D_2O - H_2O coolant for similar reasons. k_∞ peaks at around $DH/HM \approx 10$. Neutron absorption in mixed D_2O - H_2O coolant begins to play a dominant role at a lower value of DH/HM (compared to H/HM for the H_2O coolant) due to the substantial degradation in the thermal neutron utilization arising from the reduced presence of hydrogen atoms.

Figs. 5a and 6a show that the peak value of k_∞ is lower for the duplex fuel than the all- UO_2 fuel for both coolants. This is because ^{232}Th has a higher absorption cross-section than ^{238}U . The peak k_∞ of both candidate fuels with the D_2O - H_2O coolant is $\sim 2\%$ higher than with the H_2O coolant in the under-moderated region, due to the presence of large volumes (80%) of D_2O and its small neutron capture cross-section compared to H_2O coolant.

Fig. 7 shows the BOL normalized neutron flux ratio (the ratio of the flux in the mixed coolant to that in the H_2O coolant) for UO_2 fuel. It suggests that the mixed coolant yields a softer spectrum than the H_2O coolant. The ratio in the thermal range is ~ 1.65 – 1.70 , meaning that flux values in the thermal range are ~ 65 – 70% softer for the mixed coolant. Thus, the peak k_∞ values are higher for the mixed coolant due to better neutron thermalization compared to the H_2O coolant.

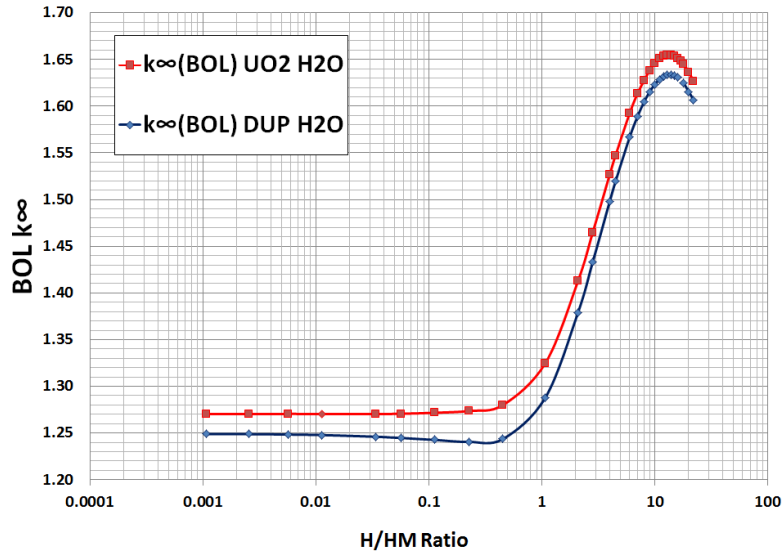
Things are different in the over-moderated region, where neutron capture in the mixed coolant dominates capture in H_2O . Fig. 8 show that BOL k_∞ values for the mixed coolant become lower than corresponding values for the H_2O coolant towards the upper end of this region.

The sensitivity of BOL k_∞ to varying fuel pin diameter (over the range 4.79–9.50 mm), while keeping the pin pitch and coolant density constant (at reference values), was investigated. Fig. 9 shows the peak BOL k_∞ values of the UO_2 and duplex fuels with H_2O coolant occur at $H/HM = 14$ and 16, respectively. Due to the presence of a strong thermal absorber (^{232}Th), the peak k_∞ of duplex fuel is 4% less than for the UO_2 fuel, which is beneficial from the perspective of reactivity control.

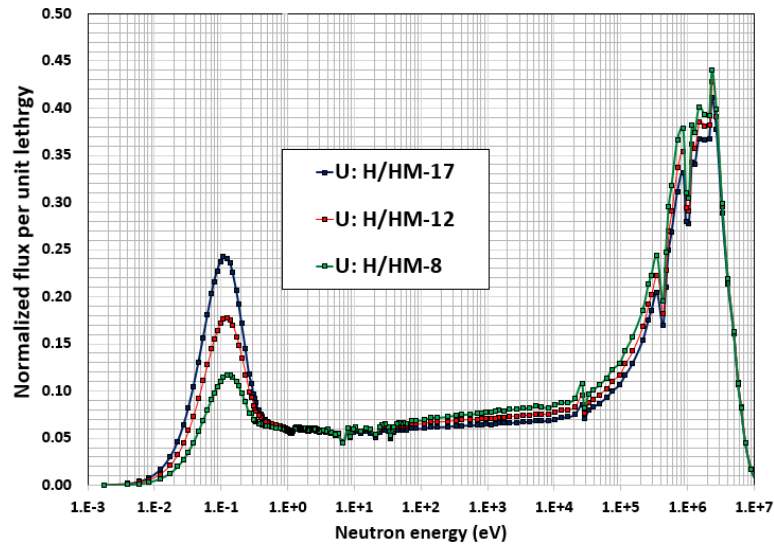
In contrast, it can be seen for the mixed coolant that peak BOL k_∞ values are reached for $DH/HM \approx 8$. At high H/HM and DH/HM ratios, BOL k_∞ values for the H_2O coolant are higher compared to those for the D_2O coolant for both the candidate fuels. This is due to the dominance of the elastic scattering cross-section of hydrogen (which is 5 times greater than that of deuterium in the slowing-down energy range).

Finally, we increased the pin pitch (over the range 9.51–23.08 mm) while keeping the fuel diameter and coolant density constant at reference values. Fig. 10 shows that the peak BOL k_∞ of the all- UO_2 fuel is 1.2% and 1.8% higher than that for the duplex fuel for the D_2O and H_2O coolants, respectively. Both candidate fuels reach peak BOL k_∞ values at an H/HM value of 14 and a DH/HM value of 9 for the D_2O and H_2O coolants, respectively.

From a neutronics viewpoint it can be anticipated that with decreases in H/HM or DH/HM

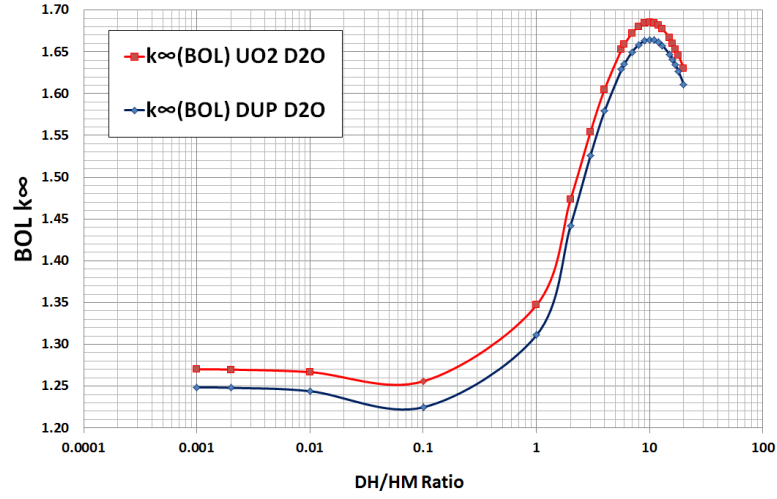


(a)

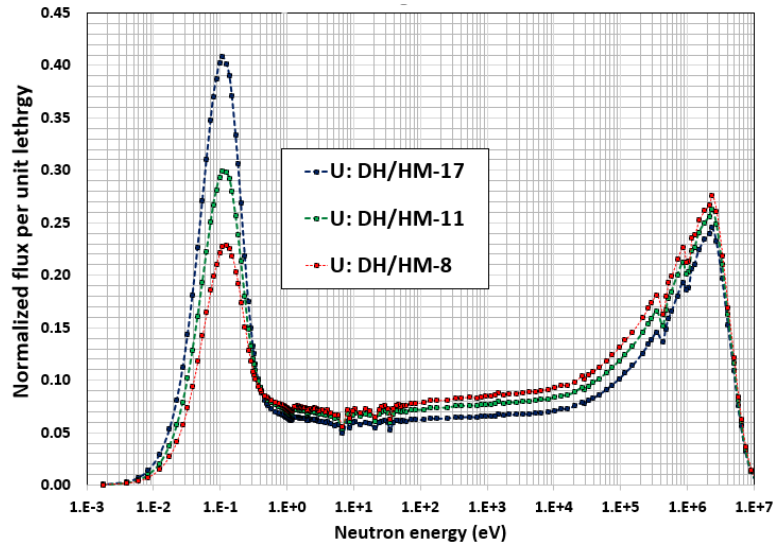


(b)

Fig. 5. (a) Initial k_{∞} as a function of H/HM by varying coolant density. (b) Neutron spectra normalized per unit flux at BOL by varying H₂O density for UO₂ fuel – H/HM values of 8, 12 and 17 are shown.



(a)



(b)

Fig. 6. (a) Initial k_{∞} as a function of DH/HM by varying coolant density. (b) Neutron spectra normalized per unit flux at BOL by varying D₂O-H₂O density for UO₂ fuel – DH/HM values of 8, 11 and 17 are shown.

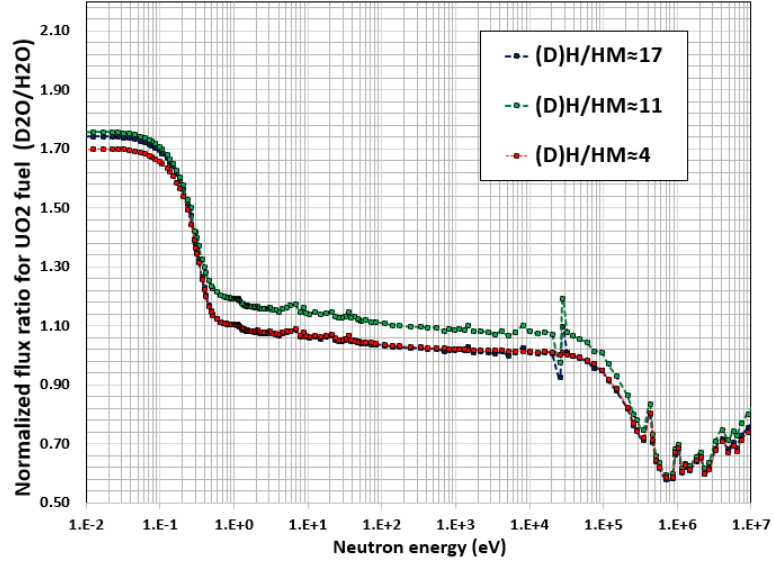


Fig. 7. Normalized neutron flux ratios ($D_2O-H_2O:H_2O$ coolant) for UO_2 fuel at BOL.

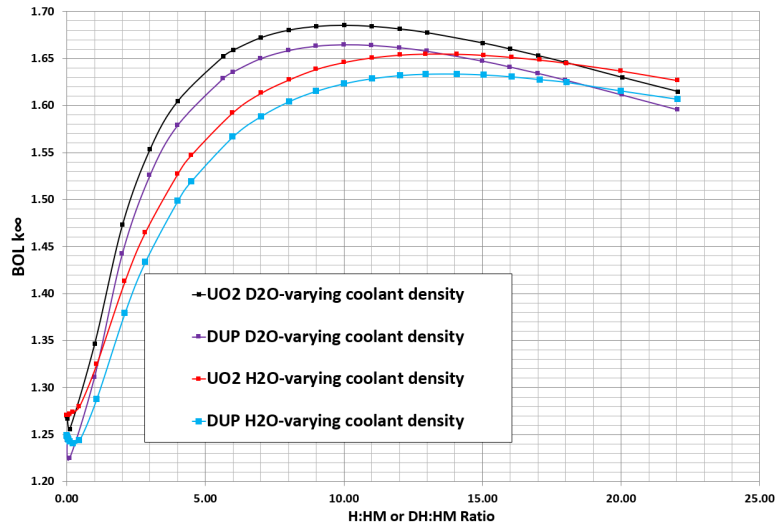


Fig. 8. BOL k_{∞} as a function of H/HM or DH/HM for all- UO_2 and duplex fuels by varying coolant density.

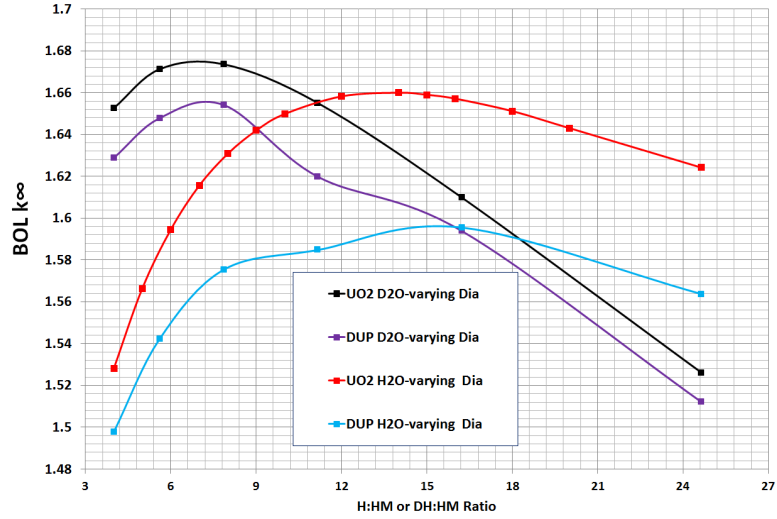


Fig. 9. BOL k_{∞} as a function of H/HM or DH/HM by varying fuel diameter (standard pitch).

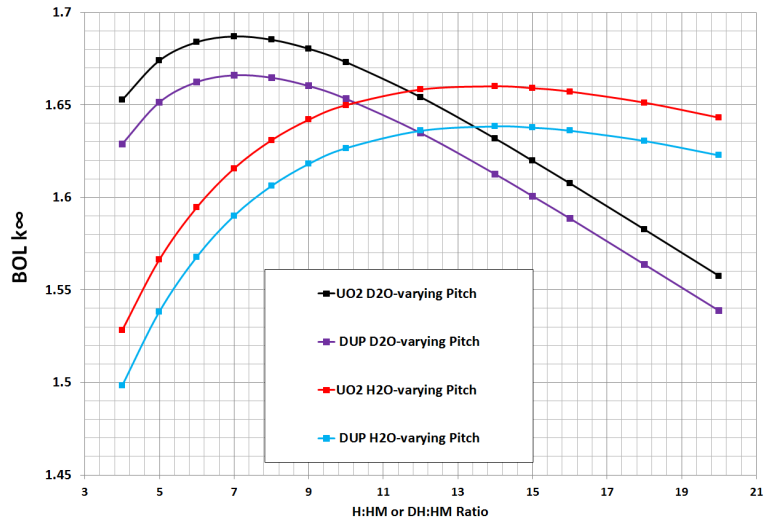


Fig. 10. BOL k_{∞} as a function of H/HM or DH/HM by varying pitch (standard fuel diameter).

270 below the optimal ratios, the neutron migration length increases so that the lattice becomes
 271 ever more homogenized. The hardening of the neutron spectrum increases the resonance
 272 absorption in ^{238}U relative to ^{235}U . Thus a monotonic decrease in k_∞ with decreasing H/HM
 273 and DH/HM is observed.

274 Control requirements are largely determined by the initial reactivity, and this parametric
 275 study suggests that wetter lattices need more control. It can be concluded that BOL k_∞ is
 276 higher for the all- UO_2 fuel for both coolants, which will certainly exacerbate the reactivity
 277 control requirements for SBF operation. Conversely, the duplex candidate fuel will require
 278 less burnable absorber than the all- UO_2 fuel for reactivity suppression. Since the D_2O
 279 coolant provides higher peak BOL k_∞ for both fuels, it will require greater poison loading
 280 for reactivity suppression, although this disadvantage may be offset by the higher achievable
 281 discharge burnup that results. Since soluble boron isn't used for reactivity control, it is
 282 required to use integral fuel burnable absorber (IFBA) burnable poison as traditional poison
 283 like gadolinia and/or erbia wasn't efficient enough (Alam, 2018, Alam et al., 2015). Therefore,
 284 a high-thickness ZrB_2 IFBA poison coating is considered in order to achieve the crucial
 285 self-shielding effect, investigating coatings of $150\ \mu\text{m}$ (Alam, 2018). In our IFBA assembly
 286 design, $150\ \mu\text{m}$ adhesive coating of zirconium diboride is coated onto the outer surface of a
 287 UO_2 pellet. For the duplex fuel case, IFBA layers are applied on the outer surface of the
 288 ThO_2 region. In order to suppress high initial and through-life reactivity swing, we used
 289 boron 95% enriched in ^{10}B throughout in order to increase neutronic effectiveness. In boron
 290 95% enriched with ^{10}B , the ratio of the absorption to total cross-section $\sigma_a/\sigma_t = 0.95$, and
 291 therefore boron is an approximately black absorber. When incorporated into ZrB_2 (density:
 292 $6.5\ \text{g}/\text{cm}^3$), it has a macroscopic absorption cross-section of $\Sigma = 297\ \text{cm}^{-1}$, and therefore a
 293 mean free path λ of $\sim 34\ \mu\text{m}$ (Otto, 2013, Alam, 2018, Alam et al., 2015). As a result, 150
 294 μm coating has poison layer with thickness greater than 3λ and these high-thickness poison
 295 layers can therefore intercept at least $\sim 95\%$ of incident neutrons. In addition, the existing
 296 subassembly design has 16 guide-tubes for loading control rods and a standard 16-rod rod
 297 cluster control assembly (RCCA) of B_4C is used. In our 112-assembly marine PWR core, 3
 298 banks of control rods (A, B and C) are used for power maneuvering and 3 other banks (SA,
 299 SB and SC) are used for shutdown. A total of 36 rod cluster control assemblies each of 16
 300 rods are used. Finally, B_4C control rod bank banks are used for obtaining criticality over life
 301 (Alam, 2018).

302 3.2. Achievable discharge burnup

303 We now examine the reactivity-limited achievable discharge burnup (B_D) as a function
 304 of H/HM and DH/HM. B_D is defined from the burnup value on the depletion curve (k_∞
 305 vs. burnup) where $k_\infty = 1$, i.e. leakage is not considered in this analysis. The sensitivity of
 306 B_D is observed for varying coolant density, fuel pin diameter and pin pitch. Figs. 11 and 12
 307 show that the duplex fuel can achieve up to $\sim 2\%$ more discharge burnup compared to the
 308 UO_2 fuel for both coolants by varying fuel pin diameter (over the range $4.79\ \text{mm}$ – $9.50\ \text{mm}$)
 309 and pin pitch (over the range 12.65 – $23.08\ \text{mm}$).

310 In contrast, the duplex fuel can achieve $\sim 7\%$ higher discharge burnup than the UO_2
 311 fuel by varying the coolant density (over the ranges 2.0×10^{-3} – $3.90\ \text{g}/\text{cm}^3$ (for H_2O) and

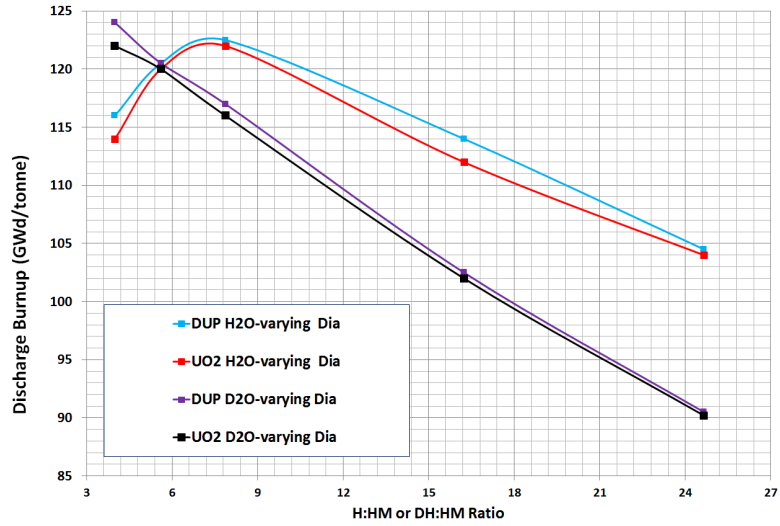


Fig. 11. B_D as a function of H/HM or DH/HM by varying fuel diameter (standard pitch).

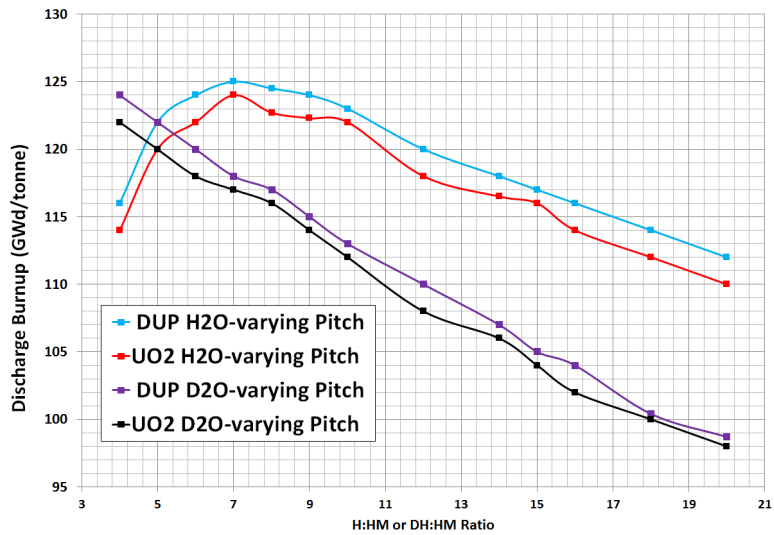


Fig. 12. B_D as a function of H/HM or DH/HM by varying pitch (standard fuel diameter).

312 1.92×10^{-4} – 3.84 g/cm^3 (for the mixed coolant)), as shown in Fig. 13. This is due to
 313 the improved ‘fertile-capture-to-fissile-absorption ratio’ of duplex fuel (Fig. 14), which is
 314 advantageous for achieving better fissile accumulation potential and thus leads to higher
 315 discharge burnups.

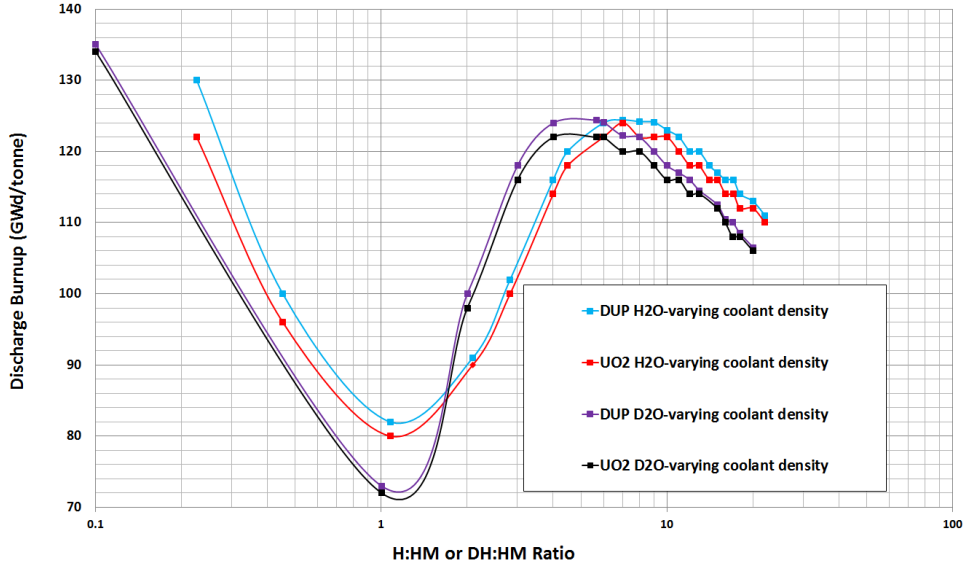


Fig. 13. B_D as a function of H/HM and DH/HM ratio by varying coolant density.

316 A slight asymmetry in B_D for various lattice optimizations can be observed. This is
 317 to be expected since the reactor physics is not entirely determined by H/HM or DH/HM.
 318 For instance, an assembly with large fuel elements and a large pitch may have the same
 319 moderator/fuel ratio as a standard assembly, but since the assembly dimensions in terms of
 320 neutron mean-free-paths are different, the neutronic behavior will not be identical in the two
 321 assemblies.

322 Figs. 11 and 12 show that, for values of (D)H/HM < 5 achieved by varying the fuel
 323 diameter or pin pitch, discharge burnups up to $\sim 8\%$ higher are obtained with the mixed
 324 coolant. For (D)H/HM values > 5 , the H_2O coolant yields higher values of B_D , with the
 325 peak occurring for H/HM ≈ 7 .

326 Fig. 13, which illustrates the effect on B_D of varying the coolant density, shows that
 327 higher B_D values are achieved with the mixed coolant for (D)H/HM values in the range from
 328 ~ 2 to 6. The highest B_D values are achieved with a hard spectrum ((D)H/HM $\ll 1$). For
 329 both coolants there is also a local maximum in B_D for each fuel at DH/HM ≈ 5 (D_2O - H_2O)
 330 and H/HM ≈ 7 (H_2O).

331 For all these lattice optimizations (varying the coolant density, fuel pin diameter and
 332 pin pitch), the duplex fuel consistently offers higher achievable discharge burnups for all
 333 moderation regimes for both coolants. It can achieve B_D values of 125 GWd/tonne with
 334 H_2O (H/HM = 7) and 124 GWd/tonne with D_2O - H_2O (DH/HM = 4), respectively, which
 335 represent $\sim 7\%$ increases in B_D compared to a reference lattice.

336 Although higher discharge burnups can be achieved with a hard spectrum ((D)H/HM \ll

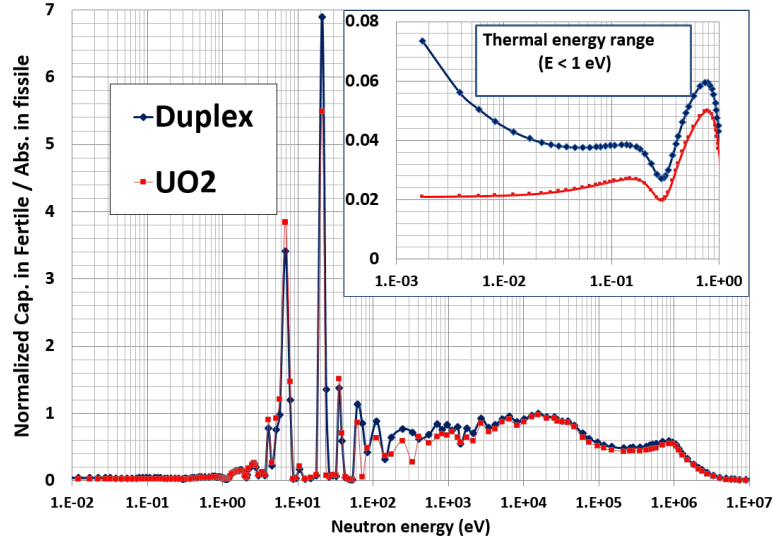


Fig. 14. Fertile-capture:fissile-absorption ratios at BOL.

337 1), the analysis of initial reactivity in Sect. 3.1 showed BOL k_{∞} values are significantly lower
 338 in this moderation regime.

339 3.3. Conversion ratio

340 The relationship between discharge burnup and initial reactivity can be explained using
 341 the concept of conversion ratio (CR), which measures the ratio of the fuel's end-of-life (EOL)
 342 and BOL fissile content. The variation of the 'achievable discharge burnup' can be understood
 343 using the linear reactivity model (Driscoll et al., 1990). Using this model, the discharge
 344 burnup in single-batch operation is determined by the initial reactivity and the slope of the
 345 k_{∞} -burnup characteristic, which is proportional to $(1/CR)$ (Xu and Driscoll, 1997). Here, the
 346 BOL CR is calculated as a function of (D)H/HM by varying coolant densities while keeping
 347 the fuel diameter and pin pitch constant (at reference values) over the range of moderation
 348 regimes. It can be observed from Fig. 15 that overall the CR decreases as (D)H/HM increases,
 349 implying that the net fissile content declines faster with increasing moderation. By looking
 350 at the figures for initial reactivity (Figs. 8, 9 and 10) and CR (Fig. 15), the behavior of
 351 'achievable discharge burnup' (Figs. 11, 12 and 13) is elucidated. In the thermal range,
 352 there is a peak in B_D , the location of which is to the right of the peak for BOL k_{∞} . In the
 353 epithermal range, B_D exhibits a minimum due to the trade-off between reduced BOL k_{∞}
 354 and improved CR. For H₂O and D₂O-H₂O cooled lattices, it is not worthwhile to operate in
 355 the epithermal range under the constraint of a once-through fuel cycle. In the fast range, the
 356 effect of CR is dominant since the initial reactivity is nearly constant.

357 Fig. 16 shows that for UO₂ fuel the neutron spectrum is gradually hardened for lower
 358 H/HM values, as expected. Since a harder spectrum facilitates the efficient conversion of
 359 fertile to fissile material, CR values are higher in the fast region than in the thermal region
 360 (as shown in Fig. 15).

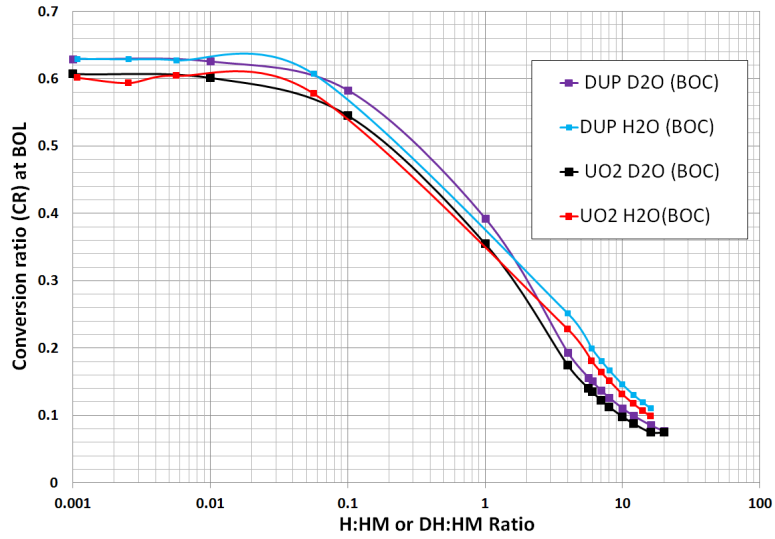


Fig. 15. BOL conversion ratio as a function of H/HM or DH/HM by varying coolant density.

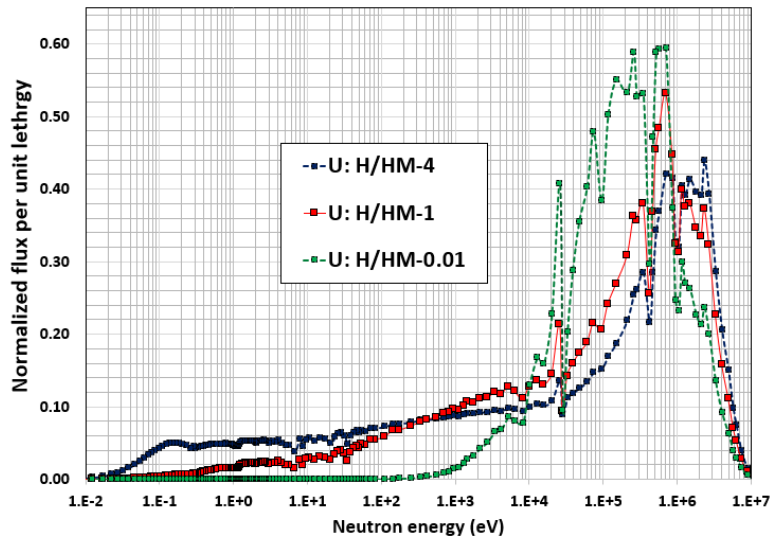


Fig. 16. Normalized flux per unit lethargy at BOL for UO₂ fuel at different H/HM by varying coolant density – H/HM values of 0.01, 1 and 4 are shown.

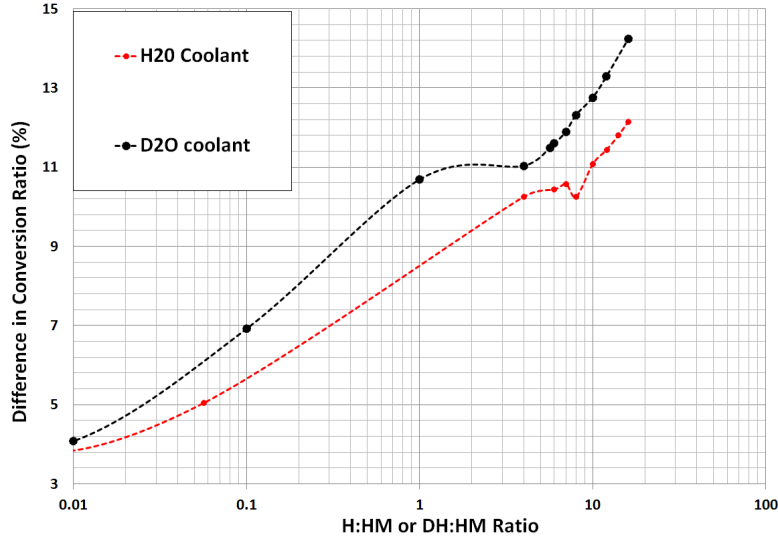


Fig. 17. Difference (%) in conversion ratio between duplex and UO_2 fuels as a function of H/HM or DH/HM by varying coolant density.

361 A higher CR is often a design goal. Fig. 17 shows that the CR of the duplex fuel is $\sim 3\%$,
 362 $\sim 8\%$ and $\sim 10\%$ higher than that of the all- UO_2 fuel in the fast, epithermal and thermal
 363 energy ranges, respectively, for both coolants, thus explaining the higher discharge burnup
 364 capability of the duplex fuel.

365 For both fuels, CR is higher for the mixed coolant in the under-moderated region but
 366 these values fall dramatically in the over-moderated region ($\text{DH}/\text{HM} > 6$), and in that
 367 moderation regime are exceeded by the CR values for the H_2O coolant.

368 The higher CR of the duplex fuel could facilitate a longer core life, which is a desirable
 369 feature for our marine core. The higher CR also results in a smaller reactivity swing between
 370 BOL and EOL, which makes the task of reactivity control of the SBF core easier.

371 4. Evaluation of the MTC and Safety Perspective

372 It is important to observe the effect of the H/HM and DH/HM on MTC and how
 373 temperature changes in the moderator affect overall reactivity. In our SBF marine core,
 374 since the coolant is also the moderator, an increase in reactor power will heat the moderator
 375 and reduce the density of moderator atoms via thermal expansion. Thus, an increase in
 376 temperature reduces the H/HM and DH/HM values. This affects the core's reactivity
 377 primarily through two distinct, but antagonistic mechanisms (Otto, 2013, Xu, 2003):

- 378 1. As the density of moderator decreases, the neutrons have fewer elastic collisions before
 379 entering the fuel. They are more likely to enter the fuel in the epithermal energy
 380 range and be absorbed in the fuel's resonances. This decreases the resonance escape
 381 probability and thus lowers k_∞ .
- 382 2. As the density of the moderator decreases, thermal neutrons are less likely to be
 383 parasitically captured in the moderator. This increases the thermal utilization factor

384 and thus also k_∞ .

385 This has important consequences for reactivity stability and inherent safety. When
 386 the first effect outweighs the second, the reactor is under-moderated, and an increase in
 387 temperature will decrease reactivity and stabilize the reactor. However, if the second effect
 388 outweighs the first, the reactor is over-moderated, and a temperature rise will further increase
 389 reactivity and power, leading to positive feedback. Any ‘optimization’ of the lattice geometry
 390 must not breach this threshold and undermine this inherent stability.

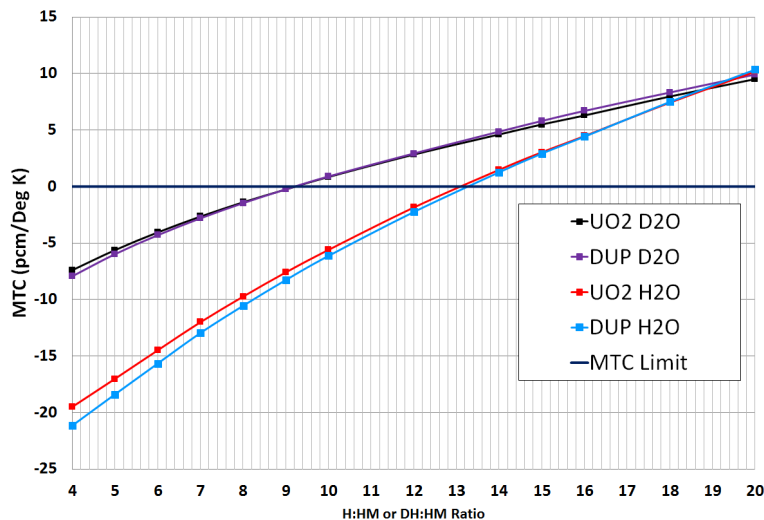


Fig. 18. MTC as a function of H/HM or DH/HM by varying pin pitch.

391 To evaluate α_M , the MTC, we calculate the BOL reactivity (ρ) for an assembly in two
 392 different conditions: first, at the standard moderator temperature (T) of 580 K, and second,
 393 with a moderator temperature ($T + \Delta T$) of 590 K (and an appropriately adjusted water
 394 density). Taking $\alpha_M \approx \Delta\rho/\Delta T$, we plot α_M against (D)H/HM in Fig. 18. MTC was
 395 investigated by varying pin pitch (over the ranges 11.54–19.94 mm (for H₂O) and 12.65–23.08
 396 mm (for the mixed coolant)), while keeping the fuel pin diameter and coolant density constant
 397 at reference values.

398 SBF operation offers potential safety in the presence of negative MTC over the entire
 399 core life. Fig. 18 shows that except at very high (D)H/HM values the MTC is lower (more
 400 negative) for the H₂O coolant. For both fuels, the upper limit on DH/HM (for negative
 401 MTC) for the mixed coolant is ~ 9 and on H/HM for H₂O it is ~ 13 . For both coolants, for
 402 (D)H/HM values giving negative MTC, the MTC of the duplex fuel is slightly more negative
 403 than that of the UO₂ fuel, more so for H₂O.

404 It is important addressing that since this neutronic study has been performed for the
 405 poison-free candidate fuels, the power peaking factors (PPF) won’t represent the true values
 406 as higher burnable poison loading and control rods will be required to suppress the reactivity
 407 for this SBF operation (Alam, 2018, Alam et al., 2015). High thickness IFBA provides
 408 different PPF values than the poison-free fuel and might deteriorate the PPFs. Therefore,
 409 PPF hasn’t been considered in this paper. In addition, peak cladding temperature calculation

410 for the poison-free fuels will be misleading since it is required to perform safety analyses
411 for the hottest channel to observe whether all operational safety criteria are met (Alam,
412 2018, Oliveira, 2016, Todreas and Kazimi, 2012). Through-life hottest channel is identified
413 by finding the pin with the highest power (Todreas and Kazimi, 2012), which is seriously
414 influenced by burnable poison and control rods. Therefore, peak cladding temperature hasnt
415 been considered in this parametric neutronic analyses of poison-free fuels. However, in
416 order to confirm that all the thermal-hydraulic safety constraints are satisfied for both the
417 candidate fuels, 3D neutronic/thermal-hydraulic hot channel analysis has been performed
418 and our study confirmed that thermal-hydraulic design requirements for both the candidate
419 fuels can be met (Alam, 2018).

420 5. Conclusions

421 This parametric neutronics study shows that, for the candidate fuels for use in a SBF,
422 civil marine SMR core considered

- 423 • A higher discharge burnup is achievable in either a wetter-than-normal or much dryer-
424 than-normal lattice, while epithermal lattices are distinctly inferior performers.
- 425 • D₂O-H₂O coolant is effective for the drier lattices in terms of achieving higher discharge
426 burnup, whereas H₂O coolant is effective for the wetter lattices.
- 427 • Candidate fuels with D₂O-H₂O coolant would require higher poison loadings than with
428 H₂O coolant due to their higher initial reactivity.
- 429 • The duplex fuel configuration offers higher discharge burnup potential for all moderation
430 regimes for both coolants due to its higher conversion ratio.
- 431 • The duplex fuel lattice would also require less burnable absorber to suppress initial
432 excess reactivity than the all-UO₂ fuel.

433 Future work will include the consideration of alternative cladding materials (e.g. ODS-type
434 steel and SiC) for very high burnup fuels and coupled neutronic-thermal-hydraulic studies for
435 heavy water coolants. Since power density is an important figure of merit and characterizes
436 design performance of marine propulsion cores, future work will also focus on the design of a
437 high power density core that fulfills the objective of providing 15 EFPY life.

438 References

- 439 Alam, S.B., 2018. The Design of Reactor Cores for Civil Nuclear Marine Propulsion. Ph.D. thesis. University
440 of Cambridge. Cambridge, UK.
- 441 Alam, S.B., Almutairi, B., Kumar, D., Goodwin, C.S., Alameri, S.A., 2018a. 3D modeling of Reduced-
442 Moderation Water Reactor lattice for P₀ and P₁ scattering approximations using deterministic and monte
443 carlo codes, in: Proc. 2018 Pacific Basin Nuclear Conference (PBNC 2018), San Francisco, CA, USA. pp.
444 285–294.

- 445 Alam, S.B., Almutairi, B., Kumar, D., Goodwin, C.S., Alameri, S.A., 2018b. Convergence studies using
446 method of characteristics solver for the Reduced-Moderation Water Reactor model, in: Proc. 2018 Pacific
447 Basin Nuclear Conference (PBNC 2018), San Francisco, CA, USA. pp. 119–128.
- 448 Alam, S.B., Goodwin, C.S., Parks, G.T., 2019. Assembly-level analyses of accident-tolerant cladding concepts
449 for a long-life civil marine SMR core using micro-heterogeneous duplex fuel. *Progress in Nuclear Energy*
450 *111*, 24–41.
- 451 Alam, S.B., Lindley, B.A., Parks, G.T., 2015. Feasibility study of the design of homogeneously mixed
452 thorium-uranium oxide and all-uranium fueled reactor cores for civil nuclear marine propulsion, in: Proc.
453 ICAPP 2015, Nice, France. pp. 1918–1927.
- 454 Alam, S.B., Lindley, B.A., Parks, G.T., 2016. Neutronic performance of high power density marine propulsion
455 cores using UO_2 and microheterogeneous $\text{ThO}_2\text{-UO}_2$ duplex fuels, in: Proc. PHYSOR 2016, Sun Valley,
456 Idaho, USA. pp. 3519–3531.
- 457 Alam, S.B., Ridwan, T., Parks, G.T., Almutairi, B., Goodwin, C.S., 2018c. High power density reactor
458 core design for civil nuclear marine propulsion. Part I: Assembly-level analysis, in: Proc. PHYSOR 2018,
459 Cancun, Mexico. pp. 46–57.
- 460 Alam, S.B., Ridwan, T., Parks, G.T., Almutairi, B., Goodwin, C.S., 2018d. High power density reactor core
461 design for civil nuclear marine propulsion. Part II: Whole-core analysis, in: Proc. PHYSOR 2018, Cancun,
462 Mexico. pp. 58–69.
- 463 Almutairi, B., Alam, S.B., , Goodwin, C.S., Usman, S., 2018. Benchmarking calculation of a soluble-boron-free
464 SMR lattice model using deterministic, hybrid monte carlo and monte carlo codes, in: Proc. 2018 Pacific
465 Basin Nuclear Conference (PBNC 2018), San Francisco, CA, USA. pp. 136–145.
- 466 Brown, N.R., Worrall, A., Todosow, M., 2017. Impact of thermal spectrum small modular reactors on
467 performance of once-through nuclear fuel cycles with low-enriched uranium. *Annals of Nuclear Energy*
468 *101*, 166–173.
- 469 Carlton, J., Smart, R., Jenkins, V., 2011. The nuclear propulsion of merchant ships: aspects of engineering,
470 science and technology. *J. Mar. Eng. Technol.* *10*, 47–59.
- 471 Clayton, J., 1993. The Shippingport Pressurized Water Reactor and Light Water Breeder Reactor. Technical
472 Report WAPD-T-3007. Westinghouse Electric Corporation, Bettis Atomic Power Laboratory. West Mifflin,
473 Pennsylvania, USA.
- 474 Driscoll, M.J., Downar, T.J., Pilat, E.E., 1990. The Linear Reactivity Model for Nuclear Fuel Management.
475 American Nuclear Society, La Grange Park, IL.
- 476 Engelder, T.C., 1961. Spectral Shift Control Reactor Basic Physics Program: Critical Experiments on
477 Lattices Moderated by $\text{D}_2\text{O-H}_2\text{O}$ Mixtures. volume 1231. Office of Technical Services.
- 478 Galperin, A., Shwageraus, E., Todosow, M., 2002. Assessment of homogeneous thorium/uranium fuel for
479 Pressurized Water Reactors. *Nucl. Technol.* *138*, 111–122.
- 480 Harvey, C., 2010. At sea over naval HEU: Expanding interest in nuclear propulsion poses proliferation
481 challenges. *Nuclear Threat Initiative* *29*.
- 482 Hirdaris, S., Cheng, Y., Shallcross, P., Bonafoux, J., Carlson, D., Prince, B., Sarris, G., 2014. Considerations
483 on the potential use of nuclear small modular reactor (SMR) technology for merchant marine propulsion.
484 *Ocean Eng.* *79*, 101–130.
- 485 Hutt, P., 1992. Overview Functional Specification of PANTHER: A Comprehensive Thermal Reactor Code
486 for Use in Design, Assessment and Operation. PANTHER/FSPEC/OVERVIEW 2.0, Nuclear Electric plc,
487 Barnwood, UK.
- 488 Ippolito, T.D., 1990. Effects of variation of uranium enrichment on nuclear submarine reactor design. Master’s
489 thesis. Massachusetts Institute of Technology.
- 490 Kazimi, M., Czerwinski, K., Driscoll, M., Hejzlar, P., Meyer, J., 1999. On the Use of Thorium in Light
491 Water Reactors. Technical Report MIT-NFCR-016. Department of Nuclear Engineering, Massachusetts
492 Institute of Technology. Cambridge, MA.
- 493 Kim, J.C., Kim, M.H., Lee, U., Kim, Y.J., 1998. Nuclear design feasibility of the soluble boron free PWR
494 core. *J. Korean Nucl. Soc.* *30*, 342–352.
- 495 Kramer, A., 1962. Nuclear Propulsion for Merchant Ships. US Atomic Energy Commission, Washington, DC.

496 Kusunoki, T., Odano, N., Yoritsune, T., Ishida, T., Hoshi, T., Sako, K., 2000. Design of advanced integral-type
497 marine reactor, MRX. Nucl. Eng. Des. 201, 155–175.

498 Leppänen, J., Pusa, M., 2009. Burnup calculation capability in the PSG2/Serpent Monte Carlo reactor
499 physics code, in: Proc. Int. Conf. Advances in Mathematics, Computational Methods, and Reactor Physics,
500 Saratoga Springs, NY.

501 Long, D., Richards, S., Smith, P., Baker, C., Bird, A., Davies, N., Dobson, G., Fry, T., Hanlon, D., Perry, R.,
502 Shepherd, M., 2015. MONK10: A Monte Carlo code for criticality analysis, in: Proc. Int. Conf. Nuclear
503 Criticality Safety (ICNC 2015), Charlotte, NC. pp. 923–935.

504 Ma, C., Von Hippel, F., 2001. Ending the production of highly enriched uranium for naval reactors. Nonprolif.
505 Rev. 8, 86–101.

506 MacDonald, P., Lee, C., 2004. Use of thorium-uranium fuels in PWRs: A general review of a NERI project to
507 assess feasible core designs, economics, fabrication methods, in-pile thermal/mechanical behavior, and
508 waste form characteristics. Nucl. Technol. 147, 1–7.

509 McCord, C., 2013. Examination of the proposed conversion of the US Navy nuclear fleet from highly enriched
510 Uranium to low enriched Uranium. Master's thesis. Massachusetts Institute of Technology.

511 Nagy, M., Aly, M., Gaber, F., Dorrah, M., 2014. Neutron absorption profile in a reactor moderated by
512 different mixtures of light and heavy waters. Annals of Nuclear Energy 72, 487–496.

513 Newton, T., Hosking, G., Hutton, L., Powney, D., Turland, B., Shuttleworth, E., 2008. Developments within
514 WIMS10, in: Proc. PHYSOR 2008, Interlaken, Switzerland.

515 Oliveira, R., 2016. Neutronic Thermal-Hydraulic Coupling of 3D MoC WIMS and Sub-channel Analysis
516 COBRA-EN Codes. Master's thesis. Department of Engineering, University of Cambridge. Cambridge,
517 UK.

518 Otto, R.T., 2013. Core Optimization in a Thorium-based Civil Marine Propulsion Reactor. Master's thesis.
519 Department of Engineering, University of Cambridge.

520 Ragheb, M., 2012. Nuclear marine propulsion. University of Illinois at Urbana-Champaign .

521 Sawyer, G., Shirley, J., Stroud, J., Barlett, E., McKesson, C., 2008. Analysis of high-speed trans-pacific
522 nuclear containership service. USA: General Management Partners LLC .

523 Schinas, O., Stefanakos, C.N., 2012. Cost assessment of environmental regulation and options for marine
524 operators. Transport. Res. C-Emer. 25, 81–99.

525 Shwageraus, E., Zhao, X., Driscoll, M.J., Hejzlar, P., Kazimi, M.S., Herring, J.S., 2004. Microheterogeneous
526 thorium-uranium fuels for pressurized water reactors. Nucl. Technol. 147, 20–36.

527 Tochiwara, H., Komano, Y., Ishida, M., Narukawa, K., Umeno, M., 1998. Nuclear design for mixed moderator
528 PWR. Progress in Nuclear Energy 32, 533–537.

529 Todosow, M., Galperin, A., Herring, S., Kazimi, M., Downar, T., Morozov, A., 2005. Use of thorium in light
530 water reactors. Nucl. Technol. 151, 168–176.

531 Todreas, N.E., Kazimi, M.S., 2012. Nuclear systems. vol. 1, thermal hydraulic fundamentals. FL: CRC Press,
532 Boca Raton, USA.

533 Winters, J.W., 2004. AP1000 Design Control Document. Westinghouse Electric Company LLC, Pittsburgh,
534 PA.

535 Xu, Z., 2003. Design strategies for optimizing high burnup fuel in Pressurized Water Reactors. Ph.D. thesis.
536 Massachusetts Institute of Technology. Cambridge, MA.

537 Xu, Z., Driscoll, M., 1997. Neutron spectrum effects on burnup, reactivity, and isotopics in UO₂/H₂O lattices.
538 Nucl. Sci. Eng. 141, 175–189.

539 Zhao, X., 2001. Micro-heterogeneous Thorium Based Fuel Concepts for Pressurized Water Reactors. Ph.D.
540 thesis. Massachusetts Institute of Technology. Cambridge, MA.